Scientific Journal for the Faculty of Science-Sirte University Vol. 4, No. 2 (2024) 1-8

Scientific Journal for the Faculty of Science-Sirte University

Journal home page: http://journal.su.edu.ly/index.php/JSFSU/index

DOI: 10.37375/issn.2789-858X

Synthesis, Characterization and Application of Goethite as an Adsorbent for Uranyl (VI) ion from its Aqueous Solutions

Arabab A. Algadi[1], Ragiab A. M. Issa[2], Farag Z. Shtewi[1] and Hana B. A. Alhanash[3]

[1]*Libyan Academy for Higher Studies, Tripoli, Libya.*

[2]*Chemistry Department, Faculty of Education, University of Tripoli, Libya.*

[3]*Advanced Libyan Laboratory for Chemical Analysis, Tripoli, Libya.*

© SJFSSU 2024.

DOI: 10.37375/sjfssu.v4i2.2912

ARTICLE INFO:

Received 25 August 2024.

Accepted 09 October 2024.

Published 26 October 2024.

Keywords: *Goethite, Adsorption, Uranyl ion, 8-hydroxyquinoline, Isotherm.*

A B S T R A C T

Nano goethite was synthesized via chemical precipitation, characterized, and utilized in batch adsorption of uranium (VI) in aqueous solution. This study aims to investigate whether a synthetic goethite could extract uranium (VI) from aqueous solutions, and to study the adsorption isotherm models. In this work, goethite (α-FeOOH) was synthesized using Atkinson et al.'s approach, which was utilized as an adsorbent. It was essential to characterize this adsorbent material. The prepared material was characterized using Fourier transform infrared (FTIR) and X-ray diffraction (XRD). Investigation and optimization have been done on different factors that may influence uranium (VI) adsorption, such as pH, initial ion concentration, and adsorbent amount. The ideal parameters that were found were then applied to actual effluents that contained uranium (VI). The results demonstrated that more than 95% of the uranium (VI) was removed. Utilizing the Langmuir, Freundlich, and Temkin models, the data shows strong agreement with the three models. According to the Langmuir isotherm model, the highest sorption capacity of goethite was 33.3 mg/g, the Langmuir constant was -7.77 L/mg, and the separation factor was $1.29x10^{-3}$. The Freundlich constant was found to be 28.31 $(mg/g)*(L/mg)^{1/n}$, and the adsorption intensity was 2.09. The was also in agreement with the Temkin model, which shows the b_T equals 68.75 joules/mol and the KT equals 3.89 L/mg. The correlation constants were in the order of 0.982 > 0.961 > 0.872 for Langmuir, Freundlich, and Temkin, respectively, explaining that the three models show favorable fittings.

1. Introduction

A mineral is a chemical substance that forms due to geological processes and has a crystalline appearance. Two examples of iron-oxide minerals present on the Earth's surface are haematite and goethite. In the natural world, goethite (a-FeOOH) is a common oxy-hydroxide that is produced when iron-containing rocks weather (Jaiswal et al., 2013). The most significant and common type of iron oxide found in soils is goethite, a yellow earth mineral principally composed of iron hydroxide. It is found in almost all soil types. Whereas haematite (Fe_2O_3) is present in many arid and/or tropical areas. It appears that goethite forms when haematite dissolves and is exposed to fresh environmental conditions. The most prevalent and stable type of iron oxide in soil is goethite (α-FeOOH), and the distribution of soluble species in the soil is influenced by the surface chemistry of this oxide (Grossi et al. 1997).

Due to its natural abundance and intense colour, goethite was one of the first pigments used in the field of art history and is still used nowadays. Temporarily, it has new uses of wastewater treatment through heavy metal

Corresponding author: E-mail: ra.issa@uot.edu.ly

absorption (Pomies et al., 1999). Numerous methods for the laboratory preparation of goethite have been documented (Legodi and de Waal, 2006).

The four main phases of ferric oxide found in nature are ferrihydrite maghemite (γ-Fe_2O_3), lepidocrocite (γ-FeOOH), haematite (α-Fe_2O_3), and goethite (α-FeOOH), in increasing order of crystallinity (Rezig and Hadjel, 2015).

Uranium is one of the hazardous heavy elements that is produced by both nuclear power plants and human activities. In its hexavalent state, it is commonly encountered in the environment as the mobile, aqueous uranyl ion. Under optimal chemical circumstances, this ion has been discovered to be strongly sorbed onto clay minerals and metal oxides; as a result, these materials can be used for the U (VI) remediation of aqueous solutions (Han, 2007; Chisholm-Brause et al., 2001). Due to the formation of many U (VI) complexes in aqueous solutions, uranium is highly soluble in hazardous environments. The aqueous concentration of U (VI) is restricted due to its high sorption to iron oxides such as ferrite and oxide hydroxides like goethite (Yusan and Erenturk, 2011; Sherman et al., 2008).

Many different methods have been applied to estimate the uranyl ion concentration in the clear supernatant obtained from filtration or centrifugation Spectrophotometric measurement was carried out by Yusan & Erenturk (2011), and the kinetic phosphorescence analyser has been done by Waite et al. (1994). Sherman et al. (2008) used the Extended X-ray Absorption Fine Structure (EXAFS) technique to investigate the surface complexation between the uranyl ion and goethite mineral.

The speciation of uranyl ions was investigated herein, and found that UO_2^{2+} is dominated up to pH 4.5. At pH~5 mono-hydroxide form UO_2OH^+ and di-hydroxide form $(UO_2)_3(OH)_2^{2+}$ of uranyl ions are formed, at about pH 7, $(UO_2)_3(OH)_5^+$ is dominated (Zhang et al., 2019; Brenhard, 2005). Therefore, pH 4.5 was selected throughout this study.

2. Materials and Methods

2.1. Materials:

Deionized water (DIW), 19.824 g of Ferric chloride dihydrate $FeCl_3.2H_2O$ (BDH, UK) in 1L DIW, 40.0g of sodium hydroxide NaOH (BDH, UK) was dissolved in 1L DIW. A 3.5M solution of potassium hydroxide KOH (MERCK, Germany) was prepared by dissolving in 2.7125 g KOH in 1L DIW. 40.406 g of ferric nitrate nonahydrate $Fe(NO_3)_3.9H_2O$ (BDH, UK) was dissolved in 1L of DIW. To prepare 1000 mg/L as uranium (stock solution), 2.1098 g of uranyl nitrate hexahydrate $UO_2(NO_3)_3.6H_2O$ (company) was dissolved in 1L DIW. 2.5% 8-hydroxyquinoline (8-HQ) from MERCK, Germany in chloroform (CARLO ERBA, Italy) was prepared.

2.2. Preparation of goethite (α-FeOOH)

The goethite mineral was prepared according to Albuquerque et al. (2022) with some modifications. 180 mL of 3.5 M potassium hydroxide solution was added to 100 mL of 0.1 M ferric chloride dihydrate ($FeCl_3.2H_2O$) at constant stirring. When the solution becomes homogenized, the volume is completed to 2 litres with deionized water, and the stirring continued for a while. The mixture was then dried at 70 °C for three days until a yellow precipitate was observed. The precipitate was further washed several times to remove any residual chloride, then was centrifuged. The produced material was then dried at 40°C for one week.

2.3. Calibration curve

A series of standard solutions of the uranyl (VI) ions were prepared to give concentrations from 1 to 30 mg/L in a total volume of 40 mL (Issa et al., 2023). The pH value was adjusted to 4.5. Using suitable separating funnels, the solutions were then extracted using 25 mL in four aliquots of 2.5% 8-hydroxyquinoline solution in chloroform, and the final volume was brought to 50 mL in volumetric flasks. The absorbance of each solution was measured at 424 nm by using a spectrophotometer (DR 3900). The calibration curve for the concentration was then plotted against absorbance.

2.4. Adsorption methods

According to a similar work (AlHanash et al. 2022)), the batch experiments were conducted at room temperature, 3 hours contact time, 2g/L adsorbent/solution ration, except for that when the adsorbent amount was the affecting parameter. 100mg/L initial ion concentration unless this was effect, and finally, 40mL as a total volume of each batch.

2.4.1. Effect pH

The effect of pH was studied in the range 3-6, as shown in Figure 1. The highest adsorbed percentage was found at pH 4.5, at which the rest of the experiments were conducted. From Figure 1, one can also see that the adsorbed percent is reduced due to the hydroxide forms of uranyl ions, which may dominate above pH 5.

Open Access Article is distributed under a CC BY 4.0 Licence.

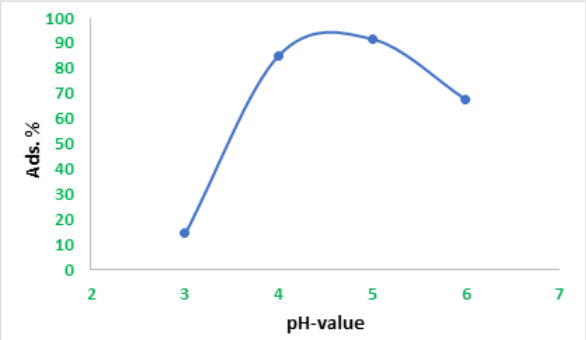

Figure 1. Effect of pH value on the adsorption of uranyl ion on goethite

2.4.2. Effect of initial ion concentration

A batch sorption was carried out at room temperature on a series of 40-mL polycarbonate centrifuge tubes. Accurate volumes of the uranyl stock solution were added to each tube to give concentrations of uranyl in the range of 50 to 200 mg/L. About 25 mL of DIW was added to each tube, and then the pH value was adjusted to 4.5. The volume was then completed to 40 mL, and 0.08 g of goethite mineral was added (2 g/L dose); the tubes were kept shaking for 3 hours. The mixtures were centrifuged at 3000 rpm for 20 minutes using the centrifuge (OHAUS), and the clear supernatant was then transferred to new tubes.

In a 50-mL separating funnel, 5 mL of the clear supernatant, 10 mL of DIW, and 10 mL of the 8-HQ solution were added to each separating funnel. The organic phase was collected in a 50-mL volumetric flask, and this separation step was repeated three times using 5 mL of the 8-HQ solution every time. The organic phases were collected for each volumetric flask, and the volume was completed to the mark using chloroform.

2.4.3. Effect of adsorbent amount

In a series of 40-mL 8-centrifuging tubes, 4 mL of the uranyl stock solution and 25 mL of DIW were added. The pH was adjusted at 4.5, and the final volume was 40 mL using DIW. A series of adsorbent doses were added to the tubes, ranging from 0.02 to 0.16 g. The tubes were perfectly sealed and kept shaking for 3 hours. The mixtures were centrifuged at 3000 rpm for 20 minutes, and the clear supernatant was separated in new tubes for further processing. The extraction step was carried on as shown in 2.4.1.

2.4.4. Mineral characterization

The synthesised goethite mineral was characterised using a Fourier transformation infrared spectrophotometer, FTIR (Agilent Cary 630 FTIR) and X-ray diffraction (Empyrean from Malvern Panalytical).

3. Results and Discussion

3.1. Mineral characterisation

The synthesized mineral was characterized using FTIR, and XRD techniques. Figure 2 shows the 4000-500 cm^{-1} FTIR spectra. Only one OH stretching mode is observed at 3119 cm1 regarding the hydroxyl stretching mode (Ruan et al., 2002); at 892 cm1 and at 792 cm1, two clear peaks appear due to the OH bending vibration mode (Villacís-García, 2015; Cambier, 1986).

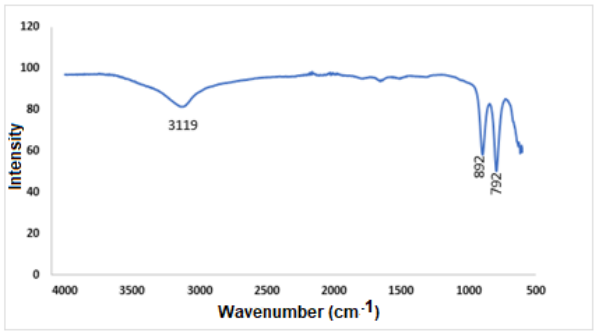

Figure 2. The FTIR spectrum of the synthesized goethite

As shown in the XRD diffractogram (Figure 3), the main peak of goethite appears at 2θ = 21.68° (d = 4.0964Å), with a relative intensity of goethite equals 36.6%. This was similar to that prepared by Hinrichs et al. (2020). However, Hinirich and his coworker do not show another high intensity peak, which may attribute to the fact that their synthesized goethite was nanoroads while ours may have been spherical and more crystalline. The highest relative intensity peak (100%) is found at 2θ = 37.16 (d = 2.4173). Data for the other peaks are given in Table 1. Figure 3 shows also that the semiquantitative composition of the prepared goethite is 28% iron oxide and 68% iron hydroxide for a structure of FeO(OH). This is in agreement with Adeoye et al. (2023).

Open Access Article is distributed under a CC BY 4.0 Licence.

Table 1: XRD date for goethite regarding diffraction angle, d-spacing and Crystal size

Pos. [°2θ]	Pos. [°θ]	Cos(θ)	Height [cts]	FWHM left [°2θ]	FWHM (RAD)	d-spacing [Å]	Rel. Int. [%]	λ(nm)	K	D (nm)
21.68	10.84	0.982	38.67	0.3936	0.00687	4.0964	36.6	0.15406	0.9	20.54
33.76	16.88	0.957	57.78	0.2362	0.00412	2.6531	54.69	0.15406	0.9	35.13
35.21	17.60	0.953	41.08	0.1574	0.00274	2.5467	38.89	0.15406	0.9	52.93
37.16	18.58	0.948	105.65	0.2755	0.00481	2.4173	100.00	0.15406	0.9	30.41
40.53	20.27	0.938	29.28	0.2362	0.00412	2.2239	27.72	0.15406	0.9	35.40
41.77	20.89	0.934	31.44	0.3149	0.00549	2.1606	29.76	0.15406	0.9	26.99
47.77	23.88	0.914	19.02	0.1574	0.002748	1.9025	18.	0.15406	0.9	55.18
51.10	25.55	0.902	20.92	0.3149	0.005498	1.7859	19.8	0.15406	0.9	27.95
53.75	26.88	0.892	71.49	0.2755	0.004810	1.7039	67.67	0.15406	0.9	32.31
54.63	27.32	0.888	24.11	0.3936	0.006872	1.6785	22.82	0.15406	0.9	22.71
57.85	28.92	0.875	17.39	0.3149	0.005498	1.5927	16.46	0.15406	0.9	28.81
59.46	29.73	0.868	64.04	0.3149	0.005498	1.5534	60.62	0.15406	0.9	29.04
61.75	30.88	0.858	50.36	0.1968	0.003436	1.5010	47.66	0.15406	0.9	47.01
64.47	32.23	0.846	37.73	0.3149	0.005498	1.4442	35.71	0.15406	0.9	29.81
66.05	33.02	0.838	15.59	0.4723	0.008246	1.4134	14.76	0.15406	0.9	20.05
67.56	33.78	0.831	12.13	0.3936	0.006872	1.3854	11.48	0.15406	0.9	24.27
69.51	34.78	0.822	21.71	0.3936	0.006872	1.3512	20.55	0.15406	0.9	24.56
71.94	35.97	0.809	24	0.3149	0.005498	1.3114	22.72	0.15406	0.9	31.16
								Average		**31.90**

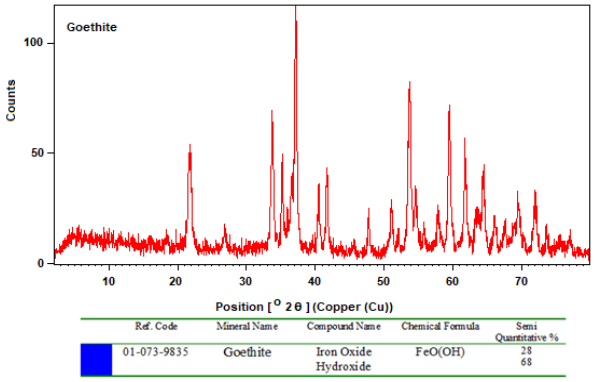

Figure 3. X-Ray diffractogram of Goethite

The crystallinity degree was calculated according to Scherrer equation (equation 1) for the data shown in Table 1 and found to be about 32 nm, which means it was a nanomaterial goethite (Adeoye et al., 2023).

$$Crystaline\ size\ (D) = \frac{K*\lambda}{\beta*Cosine\ \theta} \qquad (1)$$

Where: D is crystalline size (nm), K is the Scherrer constant (0.9), l is the wavelength for Cu $K_{1\text{-}a}$ (0.15406 nm), and β is FWHM (radians) for each peak.

3.2. Calibration curve

A calibration curve was plotted of ion concentration against absorbance. As shown in Figure 4, the calibration curve has a linear equation with a correlation coefficient R^2 = 0.9947 and a limit of detection LOD = 6.3 mg/L.

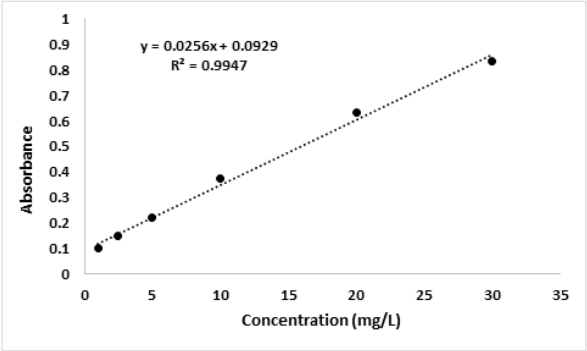

Figure 4. The calibration curve for uranyl nitrate

Open Access Article is distributed under a CC BY 4.0 Licence.

Calibration curve for standard U^{6+} solution at 1-30 mg/L. The adsorption % (Q) was calculated using equation 2, and the equilibrium adsorption capacity (q_e) was calculated using equation 3.

$$Q = \frac{C_o - C_e}{C_o} \times 100 \qquad (2)$$

$$q_e = \frac{C_o - C_e}{m(g)} \times V(L) \qquad (3)$$

Where $\mathbf{C_o}$ and $\mathbf{C_e}$ represent the initial and equilibrium concentrations, respectively, **V** is the volume of the batch solution in litres, and **m** is the adsorbent weight in grammes.

3.3. Effect of initial ion concentration

As shown in Figure 5, the percentage of uranyl ions removed was high, and the adsorption percentage decreased with increasing initial ion concentration. The adsorbed % was about 95% at 50 mg/L of ion concentration, while it reduced to almost 70% when the ion concentration became 200 mg/L. This trend is in agreement with previous studies (Issa et al., 2023; and AlHanash et al., 2022), although the percent removed of uranyl ions on diatomite and kaolinite was less.

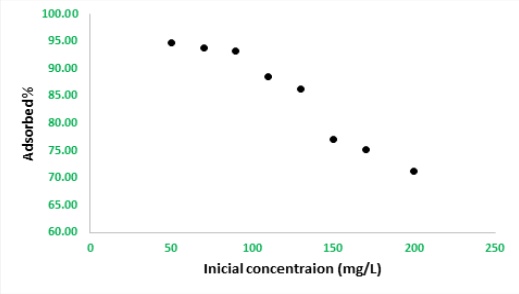

Figure 5. Effect of initial ion concentration on the removal of UO_2^{2+} by goethite.

3.4. Effect of adsorbent amount

3.4.1. Pure goethite

The effect of adsorbent amount on the adsorption of uranyl ions was studied using pure goethite (Figure 6) and aluminium-modified goethite (Al-mod-Goe); Figure 7. The adsorbed % was increased from 90% to 96% when the amount of pure goethite in the solid/solution ratio increased from 0.5 to 5 g/L (Figure 6), while it was increased from about 94% to 96% in the same solid/solution ration with the Al-mod-Goe. The equilibrium exchange capacity (q_e) was decreasing from 180 to 24 mg/g for pure goethite and from 188 to 24 mg/g for aluminium-modified goethite (Figures 6 & 7) respectively.

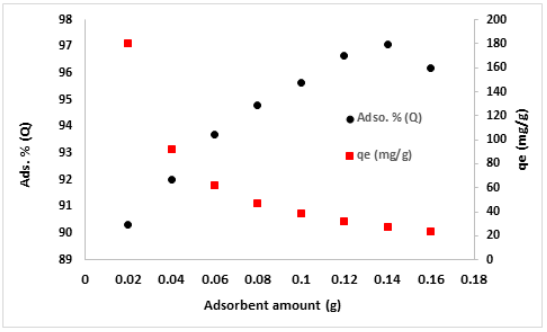

Figure 6. Effect of the amount of pure goethite on the removal of UO_2^{2+} from aqueous solution.

3.4.2. Al-Modified goethite

As shown in Figure 7, the aluminium-modified goethite does not give a significant difference with pure goethite. The adsorbed percentage is dramatically increased from about 94% (for 0.02 g adsorbent amount) to about 96% (for 0.16 g adsorbent amount). On the other hand, the equilibrium exchange capacity was decreasing from 188 to 24 mg/g for the same amounts of the adsorbent material.

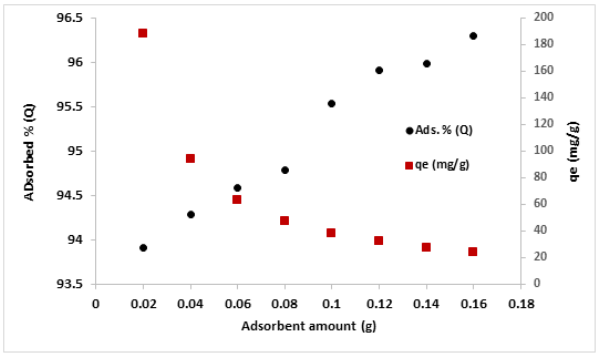

Figure 7. Effect of the amount of Al-modified goethite on the removal of UO_2^{2+} from aqueous solution.

4. Modelling

The mechanisms controlling the retention (or release) or mobility of a chemical from aqueous porous media or aquatic habitats to a solid phase at a constant temperature and pH value are frequently described by an adsorption isotherm, which is a helpful curve (Issa et al., 2023). The batch experiments that were carried out produced equilibrium isotherms for the ions. After the pH in 40 mL aliquots of 100 mg/L uranyl ion was optimised, goethite at different quantities (0.5 to 5.0 g/L) was added. According to the Langmuir isotherm, equation 4 was utilised to calculate the adsorption capacity or number of adsorbed ions in mg per unit mass of adsorbent (g). The Freundlich isotherm is based on the

Open Access Article is distributed under a CC BY 4.0 Licence.

idea that the adsorbate sticks to the heterogeneous surface of an adsorbent and applies to both monolayer (chemisorption) and multilayer adsorption (physisorption). According to Boparai et al. (2011), this model appropriately describes the adsorption data at low and intermediate concentrations on heterogeneous surfaces and permits a wide range of adsorption sites on the solid surface. Equation 4 contains the linear Freundlich equation.

$$\log(q_{max}) = \log(K_F) + \frac{1}{n}\log(C_o) \qquad (4)$$

4.1 Langmuir isotherm

The maximum uranyl ion adsorption capacity on goethite is represented by q_{max} (mg/g), and the constant K_L (L/mg) describes the attraction between the adsorbate (metal ion) and the adsorbent (mineral). Equation 5 was utilised to apply the Langmuir model to describe the isotherm.

The Langmuir model is represented linearly in Equation 6 with a good correlation coefficient R^2=0.9746 (Langmuir, 1918; Suleyman, 2020). The foundation of this concept is the hypothesis - backed by Langmuir's theory - that sorption takes place at particular homogeneous regions within the sorbent material.

$$\frac{C_e}{q_e} = \frac{C_e}{q_{max}} + \frac{1}{q_{max} \times K_L} \qquad (5)$$

By matching the plot of C_e/q_e vs. C_e (Figure 8), the Langmuir constant (K_L) was calculated using the slope and intercept of the linear equation (equation 6); refer to equations 7 and 8. The maximum adsorption capacity (q_{max}) was found to be 33.3mg/g, higher than that found by (Issa et al., 2024; Issa et al., 2023) for the adsorption of uranyl ion on diatomite. The Langmuir constant was -7.7 L/mg.

$$y = mx + c \qquad (6)$$

$$q_{max} = \frac{1}{slope} \qquad (7)$$

$$K_L = \frac{1}{q_{max} \times intercept} \qquad (8)$$

$$R_L = \frac{1}{1 + C_o \times K_L} \qquad (9)$$

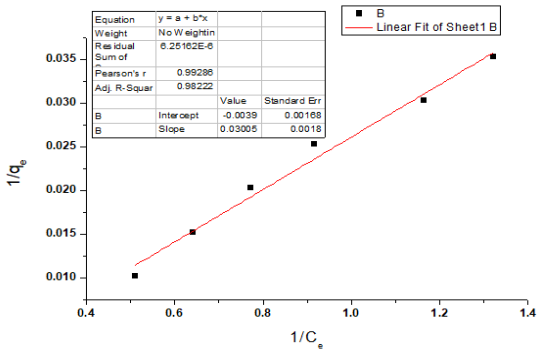

Figure 8. Langmuir isotherm model for UO_2^{2+} ion on goethite

The separation factor R_L was calculated using equation 9, where K_L is the Langmuir constant and C_o is the initial concentration. According to McKay et al., (1982), the value of R_L indicates the type of Langmuir isotherm to be irreversible (R_L = 0), linear (R_L = 1), unfavorable (R_L>1), or favorable (0 > R_L> 1). Therefore, Langmuir model in our case shows that the isotherm is favorable.

A negative K_L means that the different parts of the adsorbate interact negatively with the surface of the adsorbent, leading to desorption instead of adsorption. The Langmuir model, on the other hand, is intended to explain attractive interactions in which molecules of the adsorbate are attracted to the surface's adsorption sites (Perwitasari et al., 2021).

4.2. Freundlich isotherm

Figure 9 shows the uranyl ion's Freundlich isotherm action on goethite. The adsorption results seem to be well-represented by the Freundlich model, as evidenced by the goethite correlation constant (R^2) of 0.9610. The Freundlich constants **K_F** indicates the Freundlich adsorption capacity and **n** characterises the heterogeneity of the system. (Akl, 2021). These values are calculated from equations 10 and 11.

$$\frac{1}{n} = slope \qquad (10)$$

$$logK_F = intercept \qquad (11)$$

The behaviour of the UO_2^{2+} ion during monolayer and multilayer adsorption on goethite is described in this claim.

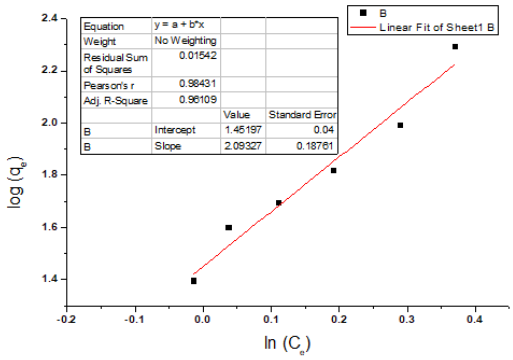

Figure 9. Freundlich isotherm model for UO_2^{2+} *ions on goethite*

From Figure 9, K_F was calculated and found to be 28.31 (mg/g)*(L/mg)$^{1/n}$ and 1/n was found to be 2.09, so the adsorption is a chemical one.

Open Access Article is distributed under a CC BY 4.0 Licence.

4.3. Temkin isotherm

Temkin isotherm model is shown in Figure 10. It gave an acceptable fitting with correlation constant R^2 = 0.872. Temkin adsorption isotherm be contingent equation 12. From Figure 10. one can say that b_T is equal to 68.75 Joul/mol and K_T is 3.89 L/mg. These values were much higher than that studied for Congo red on alginate beads impregnated with nano-goethite (Munagapati and Kim, 2017).

$$q_e = \frac{RT}{b}\ln(K_T \times C_e) \qquad (12)$$

Where: q_e = adsorption capacity at equilibrium (mg/g^{-1}).

K_T= constant of Temkin ($L.mg^{-1}$).; R = universal gas constant ($J.mol^{-1}.K^{-1}$).

T = temperature (K). Ce = Ion final concentration in solution ($mg.L^{-1}$). ; b = Heat of adsorption ($J.mol^{-1}$).

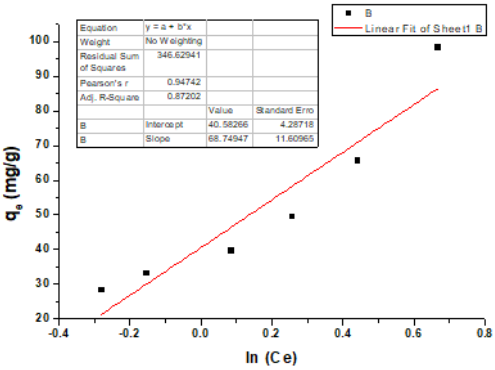

Figure 10. Temkin adsorption isotherm for UO_2^{2+} on goethite

Conclusion

This study examined the uranyl ion's adsorption on a synthetic goethite under a variety of conditions, including pH, initial ion concentration, and amount of adsorbent material. The results indicated that a pH of 4.5 was optimal. As the amount of adsorbent rises, the adsorption percentage increases, and vice versa as the starting ion concentration increases. When certain isotherm models (Langmuir, Freundlich, and Temkin) were considered, it was found that the adsorption was advantageous. The correlation constants (R^2) for Langmuir, Freundlich, and Temkin, respectively, were 0.9822, 0.9610, and 0.8720. The Langmuir model's highest exchange capacity of 33.3 mg/g suggests that goethite is a suitable adsorbent material for uranyl ion.

Conflict of Interests:

The authors declare that there are no conflict of interests.

Acknowledgment

The authors would like to express their appreciation to the Libyan Advanced Laboratory for Chemical Analysis for providing us with access to the laboratory facilities. We would also like to thank the Petroleum Research Centre for conducting the XRD analysis as part of this study.

References

Adeoye, A. O., Quadri, R. O., & Lawal, O. S. (2023). Wet synthesis, characterization of goethite nanoparticles and its application in catalytic pyrolysis of palm kernel shell in TGA. *Results in Surfaces and Interfaces*, *11*, 100118. https://doi.org/10.1016/j.rsurfi.2023.100118

Akl, Z. F. (2021). Theoretical and experimental studies on uranium (vi) adsorption using phosphine oxide-coated magnetic nanoadsorbent. *RSC advances*, *11*(62), 39233-39244.

Bernhard, G. (2005). Speciation of uranium in environmental relevant compartments. *Landbauforschung Volkenrode*, *55*(3), 139-148.

Boparai, H. K., Joseph, M., & O'Carroll, D. M. (2011). Kinetics and thermodynamics of cadmium ion removal by adsorption onto nano zerovalent iron particles. *Journal of hazardous materials*, *186*(1), 458-465.

Cambier, P. (1986). Infrared study of goethites of varying crystallinity and particle size: I. Interpretation of OH and lattice vibration frequencies. *Clay Minerals*, *21*(2), 191-200.

Cheng, T., Barnett, M. O., Roden, E. E., & Zhuang, J. (2004). Effects of phosphate on uranium (VI) adsorption to goethite-coated sand. *Environmental Science & Technology*, *38*(22), 6059-6065.

Chisholm-Brause, C. J., Berg, J. M., Matzner, R. A., & Morris, D. E. (2001). Uranium (VI) sorption complexes on montmorillonite as a function of solution chemistry. *Journal of Colloid and Interface Science*, *233*(1), 38-49.

Grossl, P. R., Eick, M., Sparks, D. L., Goldberg, S., & Ainsworth, C. C. (1997). Arsenate and chromate retention mechanisms on goethite. 2. Kinetic evaluation using a pressure-jump relaxation technique. *Environmental Science & Technology*, *31*(2), 321-326.

Open Access Article is distributed under a CC BY 4.0 Licence.

Han, R., Zou, W., Wang, Y., & Zhu, L. (2007). Removal of uranium (VI) from aqueous solutions by manganese oxide coated zeolite: discussion of adsorption isotherms and pH effect. *Journal of environmental radioactivity*, *93*(3), 127-143.

AlHanash, H. B., Issa, R. A. M., AlJabo H. A. (2022) Adsorption of UO_2^{2+} on Fibrous Cerium Phosphate and its Alanine and Arginine Intercalated Materials, *Academic Journal of Chemistry*, *7*(4): 47-54, 2022, DOI: https://doi.org/10.32861/ajc.74.47.54

Hinrichs, S., Grossmann, L., Clasen, E., Grotian genannt Klages, H., Skroblin, D., Gollwitzer, C., ... & Hankiewicz, B. (2020). Goethite nanorods: Synthesis and investigation of the size effect on their orientation within a magnetic field by SAXS. *Nanomaterials*, *10*(12), 2526. doi:10.3390/nano10122526.

Issa, R. A. M., El Amari, A. O., AlHanash, H. N., Etmimi, H. M., (2023) Removal of uranium (VI) ion from aqueous solution using kaolinite, *Kuwait Journal of Science*, (50), 609-614, https://doi.org/10.1016/j.kjs.2023.03.010.

Issa, R. A., AlHanash, H. B., Abdulsalam, M. M., Tekalli, A. A., Hamed, L. K. B., & Omran, S. A. B. (2024). Study on Natural Diatomite as an Adsorbent for Uranyl (VI) ions, Using Spectrophotometric Method. *Journal of Pure & Applied Sciences*, *23*(1), 58-63.

Jaiswal, A., Banerjee, S., Mani, R., & Chattopadhyaya, M. C. (2013). Synthesis, characterization and application of goethite mineral as an adsorbent. *Journal of Environmental Chemical Engineering*, *1*(3), 281-289. http://dx.doi.org/ 10.1016/ j. jece.2013.05.007.

Langmuir, I. (1918). The adsorption of gases on plane surfaces of glass, mica and platinum. *Journal of the American Chemical society*, *40*(9), 1361-1403.

Legodi M. A. (2008) Raman Spectroscopy Applied to Iron Oxide Pigments from Waste Materials and Earthenware Archaeological Objects, Ph D thesis submitted to the University of Pretoria.

McKay, G., Blair, H.S., and Gardner, J. R. (1982) Adsorption of dyes on chitin, J. Appl Polym Sci 27(8): 3043-3057.

Perwitasari, D. S., Pracesa, Y. A. Y., Pangestu, M. A., & Tola, P. S. (2021). Langmuir and Freundlich isotherm approximation on adsorption mechanism of chrome waste by using tofu dregs. *Nusantara Science and Technology Proceedings*, 106-112. doi: 10.11594/ nstp.2021.1417

Pomiès, M. P., Menu, M., & Vignaud, C. (1999). Red Palaeolithic pigments: natural hematite or heated goethite?. *Archaeometry*, *41*(2), 275-285.

Rezig, W., & Hadjel, M. (2015). Preparation and characterization of iron oxide modified diatomite system. *Der Pharma Chemica*, *7*(2), 5-11.

Ruan, H. D., Frost, R. L., Kloprogge, J. T., & Duong, L. (2002). Infrared spectroscopy of goethite dehydroxylation: III. FT-IR microscopy of in situ study of the thermal transformation of goethite to hematite. *Spectrochimica Acta Part A: Molecular and Biomolecular Spectroscopy*, *58*(5), 967-981.

Ruan, H. D., Frost, R. L., Kloprogge, J. T., & Duong, L. (2002). Infrared spectroscopy of goethite dehydroxylation: III. FT-IR microscopy of in situ study of the thermal transformation of goethite to hematite. *Spectrochimica Acta Part A: Molecular and Biomolecular Spectroscopy*, *58*(5), 967-981.

İnan, S. (2020). Sorption studies of europium on cerium phosphate using Box-Behnken design. *Turkish Journal of Chemistry*, *44*(4), 971-986.

Villacís-García, M., Ugalde-Arzate, M., Vaca-Escobar, K., Villalobos, M., Zanella, R., & Martínez-Villegas, N. (2015). Laboratory synthesis of goethite and ferrihydrite of controlled particle sizes. *Boletín de la Sociedad Geológica Mexicana*, *67*(3), 433-446.

Waite, T. D., Davis, J. A., Payne, T. E., Waychunas, G. A., & Xu, N. (1994). Uranium (VI) adsorption to ferrihydrite: Application of a surface complexation model. *Geochimica et Cosmochimica Acta*, *58*(24), 5465-5478.

Yusan, S. D., & Erenturk, S. A. (2011). Sorption behaviors of uranium (VI) ions on α-FeOOH. *Desalination*, *269*(1-3), 58-66.

Munagapati, V. S., & Kim, D. S. (2017). Equilibrium isotherms, kinetics, and thermodynamics studies for congo red adsorption using calcium alginate beads impregnated with nano-goethite. *Ecotoxicology and environmental safety*, *141*, 226-234.

Open Access Article is distributed under a CC BY 4.0 Licence.